MODULATION LANE MEASUREMENT OF JUPITER'S IO–B SOURCE PARAMETERS

K. Imai*, F. Reyes†, and T. D. Carr†

Abstract

In previously published work we have developed a model to explain the production of modulation lanes in the dynamic spectra of Jupiter's decametric emission. By using our model and the analysis of the curvature of the modulation lanes we have obtained the cone half–angle of the emission for the Io–B source. Our results show that the value of the cone half–angle remains at a fixed value of 60 degrees for each of the storms analyzed and that the longitude of the intersection of the active magnetic flux tube with the equatorial plane increased linearly with time. We also found that the values of the cone half–angle deduced from measurements of a few modulation lanes delineated by S–bursts is about 50 degrees, 10 degrees smaller than the cone half–angle deduced from modulation lanes of L–bursts.

1 Introduction

The Jovian decametric radiation is emitted in the X mode at frequencies approximately equal to the local electron cyclotron frequencies (f_c) from auroral–zone source regions in the lower magnetosphere of the planet (see, for example, [Carr et al., 1983], and references therein). Most of the emission originates from localized sources within a relatively narrow sector of longitude in the northern auroral zone (although there is probably a less active source region in the southern auroral zone). Radiation from the individual localized sources is emitted into similar thin–walled hollow–cone beams having relatively wide opening angle, the cone axis in each case being tangent to the magnetic field at the source. Since they are fixed to the magnetic field at the individual source locations, these hollow–cone beams corotate with the planet. Radiation from the sources can be received at terrestrial observatories only when some part of the leading or trailing sides of the hollow–cone beams are aligned with Earth. Radiation from the northern auroral zone appears in two regions of central meridian longitude (CML) that are referred to as the Source B and Source A regions. Whether the radiation is of Source B or A depends

*Department of Electrical Engineering, Kochi National College of Technology, Kochi 783–8508, Japan
†Department of Astronomy, University of Florida, Gainesville, FL 32611–2055, USA

on which side of the hollow–cone beams is aligned with Earth. The occurrence probabilities and intensities of these emissions are enormously increased if the magnetic flux tube within which the source lies was recently activated by having been swept across the Jovian moon Io as a result of the corotation of the field with the planet. The Source B and Source A emissions that have thus been greatly stimulated by Io are referred to as Io–B and Io–A emissions.

The modulation lanes in Jupiter's decametric radiation, which were discovered by Riihimaa [1968b], are groups of sloping parallel strips of alternately increased and decreased intensity in the dynamic spectral plots (i.e., in plots of intensity versus frequency and time). Extensive systematic observations of modulation lanes have been made in the frequency range 21 to 23 MHz by Riihimaa [1970; 1974; 1978]. The frequency–time slopes of the lanes can be either positive or negative, depending on which of the Jovian sources is being observed.

A number of attempts have been made over the years to establish accurately the radio source geometry and hollow–cone emission beam dimensions by modeling. Some of these results are no doubt approximately correct, but the available constraints to apply in such modeling have generally been insufficient to produce convincing results of useful accuracy. Measurements that are particularly in need of verification are the source longitudes and L–shells for the Io–B, Io–A, and non–Io–A emission regions and the opening angles and wall thicknesses of their hollow–cone emission beams. The development of the modulation lane method for the measurement of such quantities by Imai et al. [1992a; 1992b; 1997] has provided an independent and apparently relatively precise means for the verification of previous measurements by other methods (although the modulation lane measurements, like all those that have been made in other ways, are of course highly model dependent).

In the Imai et al. model for the production of modulation lanes, the lanes are assumed to be a manifestation of interference fringes from the line source consisting of the points along the axis of the Io–activated flux tube that are emitting at the different local values of f_c. The fringes are produced as a result of the passage of the multi–frequency radiation through an interference grating. This grating is a planar grid of almost equally spaced field–aligned columns of enhanced plasma density, perpendicular to the ray–paths toward Earth, located near the sub–Earth point on Io's orbit. Radiation from each of the frequencies emitted by the line source produces a set of interference fringes when it is scattered by the plasma–enhanced columns. These sets of fringes are inclined with respect to the Jovian equator. The rotation of Jupiter sweeps the inclined interference patterns for the different frequencies across Earth, producing the modulation lanes in the observed dynamic spectra. For a given set of the adjustable parameters the model produces a plot of frequency versus time for a single modulation lane. This modeled plot is then compared with the observed plot of a particular lane, and adjustments in the assumed parameters for subsequent improved plots are made until the best fit is obtained. The final result thus consists of the values of those adjustable parameters that are used to obtain the best–fitting modulation lane curve.

2 Model prediction for wide–band modulation lanes

In our previously published results on modulation lanes, most of the observational data available to us was of relatively narrow bandwidth, about 2 MHz. With modulation lanes of such a narrow bandwidth it was not possible to detect any significant curvature in the lanes; they appeared as straight lines. The modulation lanes present in the few available wide–band dynamic spectra did exhibit curvature, the slope increasing with time as our model predicted. The increasing slope of the frequency–time curve is the result of the non–linear relationship of the magnetic field strength B with distance along the magnetic field line. In our modeling we have assumed that the emitted frequency is very close to the local cyclotron frequency ($f_c = 2.8\ B$). In order to compute the slope of the curve we use equation (2) of Imai et al. [1997] with a fix frequency step $f_h - f_l$. As the modeling process approaches the planet (high frequency range), the distance corresponding to each frequency step decreases along the magnetic field line and therefore the projection $x_h - x_l$ becomes smaller and smaller increasing the value of the slope.

For this paper we have examined all the available published or unpublished wide–band modulation lane data (bandwidths 10 MHz, more or less) in order to determine whether the curvature predicted by our model is approximately correct. The data are from three sources: 1) the paper by Genova et al. [1981] containing observations made over two apparitions beginning in 1978 and covering the frequency range 10 to 40 MHz; 2) a group of 5 previously unpublished dynamic spectra observed by Reyes at University of Florida Radio Observatory in 1997 and 1999; and 3) a set of data observed in Finland by Riihimaa in 1987 and 1988, which is described in the next section. Careful inspection revealed that all of the wide–band modulation lanes were indeed curved, the slope always increasing with time as predicted. Figure 1 shows an example of the wide–band curved lanes from the Io–B source as observed in Florida.

3 Io–B source and beam parameters from wide–band modulation lanes

We now use our model to improve the determination of source and beam parameters from a uniform and extensive set of unpublished observational data. The observations used for this were made by Riihimaa at Aarne Karjalainen Observatory of the Department of Astronomy, University of Oulu, Finland, in 1987 and 1988, at frequencies between 20 and 32 MHz [Riihimaa, 1993]. The antenna system consisted of an array of two crossed log periodic polarimetric antennas from which, the right–hand (RH) and left–hand (LH) circularly polarized components of the radiation were obtained. The received radiation was processed and recorded by an analog acousto–optical radio spectrograph, providing frequency and time resolutions of about 70 kHz and 150 ms, respectively.

It has previously been demonstrated that the dynamic spectral characteristics of modulation lanes (other than their amplitudes) are the same for the RH and LH components if both are present [Riihimaa, 1975, 1976; Genova et al., 1981]. Thus for the present analysis only the RH component was recorded and analyzed. From the data we plotted

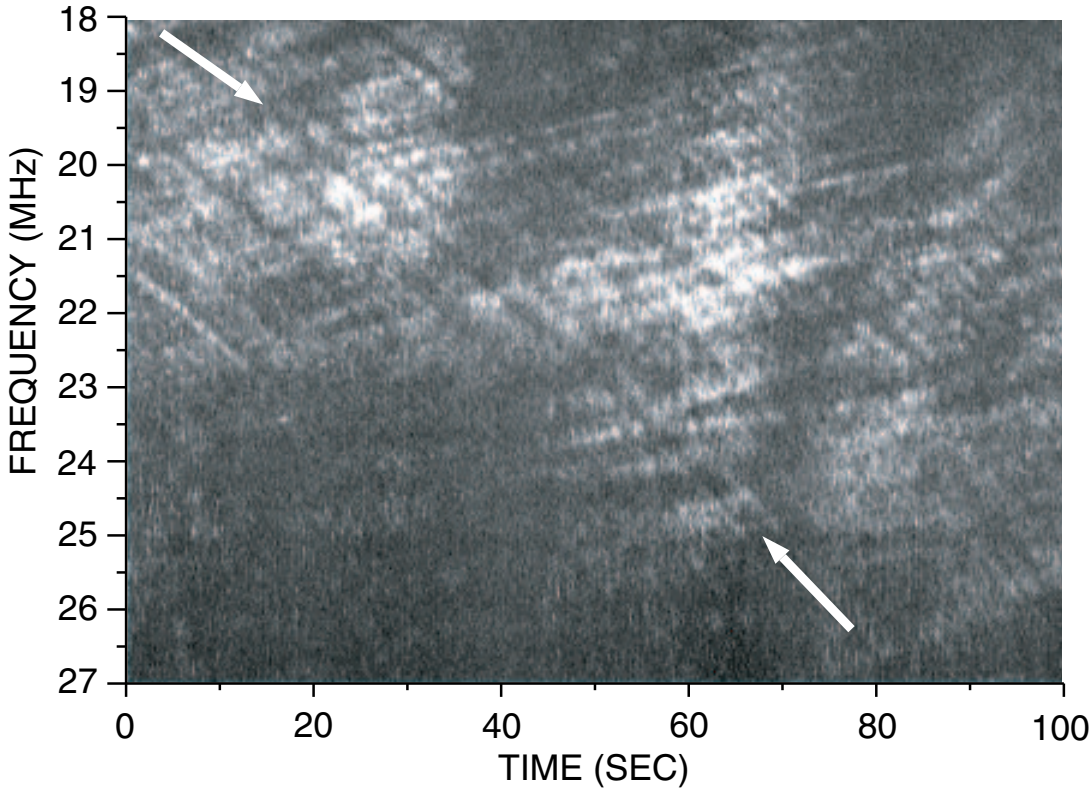

Figure 1: Wide bandwidth modulation lanes observed from the Io–B source on August 23, 1997 by the University of Florida Radio Observatory wide–band radio spectrograph. The curvature of the modulation lanes shown by the arrows is clearly seen.

43 frequency versus time curves delineating modulation lanes representative of different sections of four selected Io–B storms. The data defining each of these curves consists of 7 points, one measurement for each 2 MHz of frequency (corresponding to the points shown in Figure 3). Figure 2 indicates the locations of the four storms on the plane of System III central meridian longitude (λ_{III}) versus the orbital phase of Io (ϕ_{Io}).

The procedure used to determine the cone half–angle of the emission starts with the determination of the values of λ_{III} and ϕ_{Io} using the time of the observation. Next, a value of longitude lead angle of the source ahead of Io (α) is assumed. To calculate the longitude of the intersection of the active magnetic flux tube with the equatorial plane (θ), all the three previous values are entered in the formula $\theta = 180^o - \phi_{Io} - \alpha + \lambda_{III}$. Starting at the equator and using the value of θ, we traced a magnetic field line using the O_4 model [Acuña and Ness, 1976] toward the northern hemisphere. The location of the source (at a given frequency) is defined by the point along the magnetic field line at which the local gyrofrequency matches the observed frequency. Once the location of the source is found, we determine the cone half–angle β as the angle between the direction tangent to the magnetic field line at the source and the direction to the Earth as seen from the source.

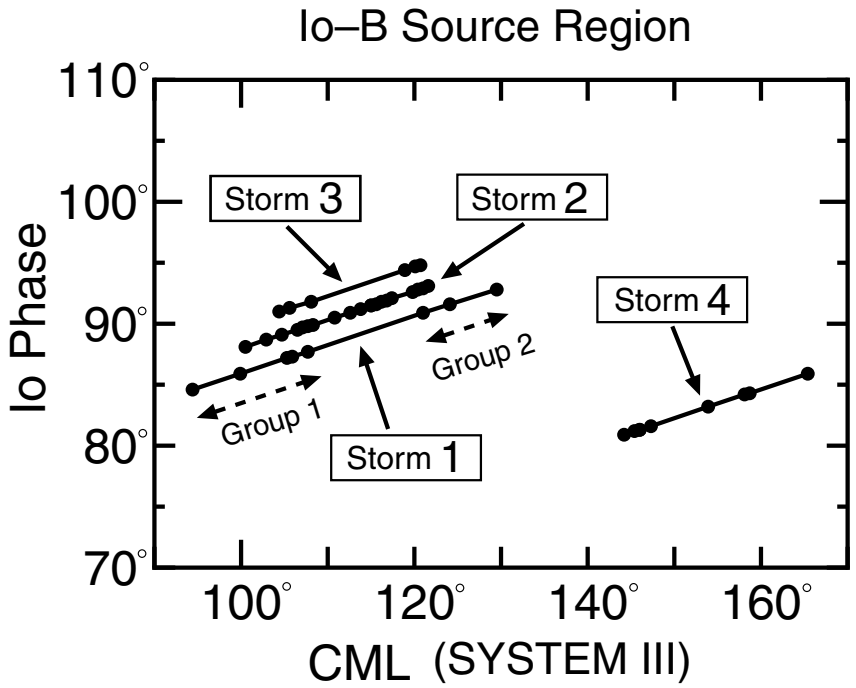

Figure 2: Plot of the locations of the four storms in the CML–Io phase plane. The filled circles indicate the location of the modulation lane events used in this analysis.

For a given value of θ, the slope of the modulation lane curve for the appropriate frequency range can be calculated using equation (2) of Imai et al. [1997]. In this analysis we calculated 24 values of slope for the frequency range between 20 and 32 MHz in 0.5 MHz steps. In the frequency–time plane, the slopes are defined by

$$SL_n = \frac{\Delta f_n}{\Delta t_n} \tag{1}$$

where n = 1,...,24. Δf_n is the frequency step (500 kHz). Δt_n is the corresponding time in seconds. To calculate the Δt_n values we use equation (1) with Δf_n=500 kHz and the already calculated SL_n values. In order to plot the modeled modulation lane in the frequency–time plane, we calculate each pair of values (f_n, t_n) for each point using

$$(f_n,\ t_n) = (20 + 0.5\ n\ ,\ \sum_{i=1}^{n} \Delta t_i\ ) \tag{2}$$

where 20 is the starting frequency in MHz and 0.5 is the frequency step in MHz. Equation (2) is used to generate each of the curves in Figure 3. Several of these curves are computed for different values of α until a good match between the curve defined by the observational points and the one generated by our model is obtained. This procedure was followed for each of the 43 sets of points defining separate modulation lanes.

Figure 3 shows a graphical example of the procedure used to match the observed curvature of the modulation lanes. The observational data points, plotted as filled circles, define

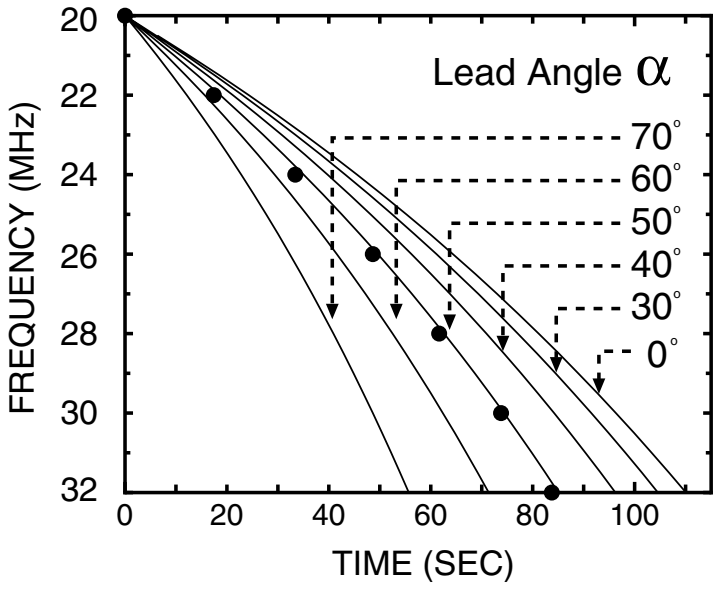

Figure 3: An example illustrating the fitting process used to obtain the value of the lead angle of α. The filled circles are plots of the frequency–time values deduced from the observed slopes. The solid lines are plots of the curves generated by the model. The best fit is obtained by the curve corresponding to a lead angle of 49^o.

this curve which consist of 7 points, one measurement for each 2 MHz of frequency. The 6 curves plotted in Figure 3 were calculated from our model for the indicated values of α. It is apparent from the figure that the modeled curve that best fits the 7 points delineating the observed modulation lane would be one corresponding to a lead angle of about 49^o.

Figure 4 shows θ and β versus CML as calculated from the lead angle values at the frequency of 23 MHz. The plot of θ as a function of CML for Storm 2 shows a clear linear increase. The interpretation of this linear increase is that the location (longitude of the intersection of the active magnetic flux tube with the equatorial plane) is continuously changing with the rotation of Jupiter. The plot of cone half–angle β for Storm 2 shows that this parameter remains constant at 60^o over a longitude range of 21^o, which corresponds to an observing time of 35 minutes. In the case of Storm 3, we see the same trend as of Storm 2. Although Storm 3 has a gap between two groups, the extrapolated line shows the same trend.

On the other hand, Storm 1 shows a different aspect in comparison with Storm 2 and 3. Storm 1 has two groups of data (labeled Group 1 and 2 in Figures 2 and 4). Both groups show a linear increase in θ with CML, however the values of θ for the second group does not fall in the extrapolation of the values of the first group. There is a clear discontinuity in θ between the two groups. The corresponding cone half–angle β for the first group is about 60^o; for the second group is about 50^o. The difference is about 10^o. In an attempt

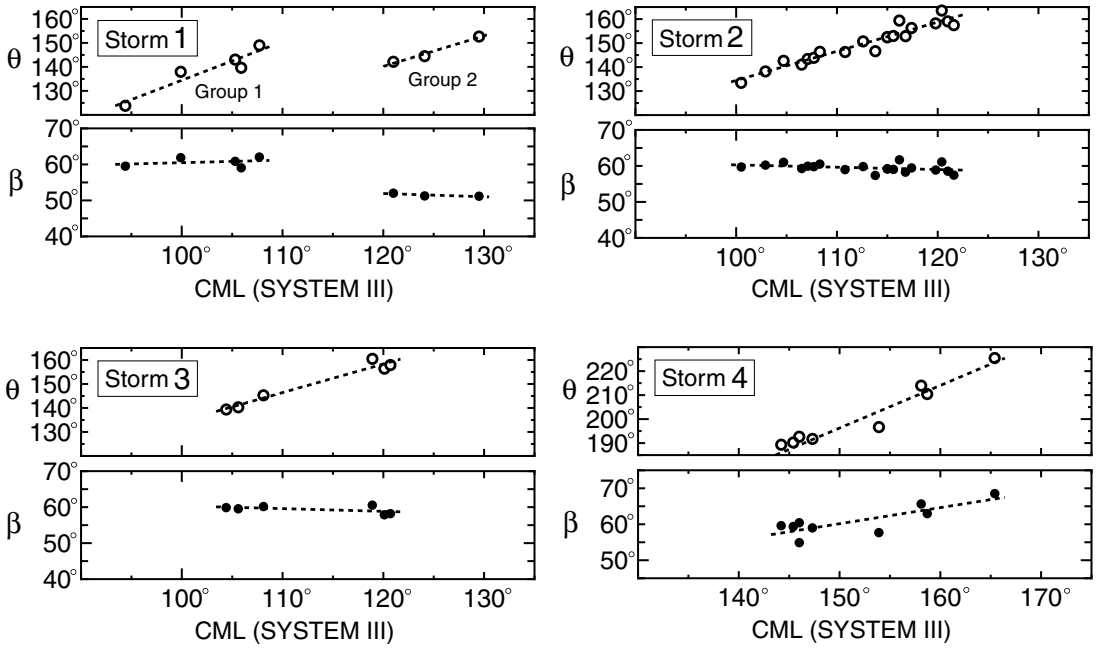

Figure 4: Plot of the derived parameters, longitude of the intersection of the active magnetic flux tube with the equatorial plane θ and cone half–angle β versus CML (System III longitude of Earth) for the four storms. The dotted lines are the linear fits to the derived values.

to try to find an explanation for this behavior we examined samples of dynamic spectra corresponding to the two groups. We found that the first group is composed only by L–bursts; the second group is composed mainly by S–bursts, with the presence of some L–bursts at lower frequency. The second group shares part of the values of θ with the first group. This would indicate that both emitting sources are located along the same active flux tube thus implying that they have two different beam cone half–angle, one being 60^o and the other 50^o. However, from our data, we can not establish if this kind of double beaming exists along all longitudes.

Storm 4 also has slightly different characteristics in comparison with Storm 2. In both storms, θ is increasing almost linearly, but the corresponding cone half–angles instead of being constant as in Storm 2, seems to be slightly increasing in Storm 4. The cone half–angle is about 60^o for the earlier part of the storm; for the latter part it increases to about 70^o. We note that the CML values (158^o–165^o) for the latter part are close to the edge of Io–B region.

In summary, we investigated 43 modulation lanes events originating in four storms. In Storm 2 and 3, we can establish that the longitude of the intersection of the active magnetic flux tube with the equatorial plane increases linearly with Jupiter's rotation. The cone half–angle seems to maintain an almost constant value of 60^o (measured at 23 MHz). This result agrees with our previous analysis made by using relatively narrow

bandwidth, 21 to 23 MHz, modulation lane data [Imai et al., 1992a; 1992b; 1997]. In Storm 1, the different cone half–angles would imply that the source beaming is different for L–bursts and S–bursts. The latter half part of Storm 4 shows a slightly larger cone half–angle, near 70^o.

4 Conclusion

For the Io–B modeling, the source and the interference screen were assumed to be on the same L–shell as Io, the screen being at the distance of Io's orbit. The best fit modeled results indicate that the half–angle of the hollow–cone beam has a fixed value of 60^o, and the longitude of the intersection of the active flux tube with Io's orbit increases linearly with time. This can be interpreted as caused by the radiation being beamed into a hollow cone with a wall thickness less than a few degrees, otherwise this kind of consistent trend can not be explained. In other words, the emission received at the Earth seems to originate from sources located in a very limited sector of longitude. During one storm the L–bursts emission was replaced briefly by S–bursts emission. At the same time, the cone half–angle changed from 60^o for L–bursts to 50^o for S–bursts, a decrease of 10^o. If this effect can be verified in future observations as a true difference between the beaming of L– and S–bursts, it will provide valuable information for use in attempts to explain the difference in the sources of the two kinds of bursts.

Acknowledgements: We are grateful to Jorma J. Riihimaa for providing the observational data points from which most of the results in this paper were calculated. We would like to thank Wesley B. Greenman for his assistance of the observations at the University of Florida Radio Observatory.

References

Acuña, M. H., and N. F. Ness, The main magnetic field of Jupiter, *J. Geophys. Res.*, **81**, 2917–2922, 1976.

Carr, T. D., M. D. Desch, and J. K. Alexander, Phenomenology of magnetospheric radio emissions, in *Physics of the Jovian Magnetosphere*, edited by A. J. Dessler, 226–284, Cambridge Univ. Press, New York, 1983.

Genova, F., M. G. Aubier, and A. Lecacheux, Modulations in Jovian decametric spectra: Propagation effects in terrestrial ionosphere and Jovian environment, *Astron. Astrophys.*, **104**, 229–239, 1981.

Imai, K., L. Wang, and T. D. Carr, A model for the production of Jupiter's decametric modulation lanes, *Geophys. Res. Lett.*, **19**, 953–956, 1992a.

Imai, K., L. Wang, and T. D. Carr, Origin of Jupiter's decametric modulation lanes, in *Planetary Radio Emissions III*, edited by H. O. Rucker, S. J. Bauer, and B. M. Pedersen, Austrian Academy of Sciences Press, Vienna, 69–90, 1992b.

Imai, K., L. Wang, and T. D. Carr, Modeling Jupiter's decametric modulation lanes, *J. Geophys. Res.*, **102**, 7127–7136, 1997.

Riihimaa, J. J., Structured events in the dynamic spectra of Jupiter's decametric radio emission, *Astron. J.*, **73**, 265–270, 1968b.

Riihimaa, J. J., Modulation lanes in the dynamic spectra of Jovian L–bursts, *Astron. Astrophys.*, **4**, 180–188, 1970.

Riihimaa, J. J., Modulation lanes in the dynamic spectra of Jupiter's decametric radio emission, *Ann. Acad. Sci. Fenn.*, **A VI**, 1–39, 1974.

Riihimaa, J. J., Polarization structure of Jupiter's decameter radio bursts, *Nature*, **255**, 210–211, 1975.

Riihimaa, J. J., Polarization patterns in the dynamic spectra of Jupiter's decametric radio bursts, *Astron. Astrophys.*, **53**, 121–129, 1976.

Riihimaa, J. J., L–bursts in Jupiter's decametric radio spectra, *Astrophys. Space Sci.*, **56**, 503–518, 1978.

Riihimaa, J. J., Decametric radio spectra of Jupiter: Modulation lanes revisited, Dept. of Astron., Univ. of Oulu, Finland, 1993.